The solution was injected towards the substrate when the valve was opened for 1.5 ms. When the DNA solution was injected perpendicularly onto the substrate, no extended DNA was observed in atomic force microscopy images. When the DNA solution was injected at a slanting angle such as 45° onto the substrate, extended DNA was observed. The *dI/dV* map was measured with lock-in detection of the a.c. tunnelling current by modulating the sample bias (0.1 V r.m.s., 1 kHz) while keeping the feedback loop active.

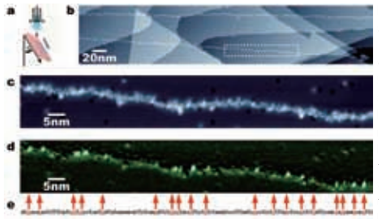

Fig. 1 Deposition and STM analysis of single-stranded M13mp18 DNA molecules on a Cu(111) surface. a, Schematic illustration of the oblique injection method. DNA strands tend to align more perpendicular than horizontal to the flow (injection) direction. The Cu(111) substrate is inclined at ~45° to the aqueous solution of DNA, which is introduced from a pulse valve. **b,** Typical wide-area image of M13mp18 (2 V, 5 pA, width 400 nm). Atomic steps in the Cu(111) substrate form a staircase surface structure. In this image, sections of M13mp18 are visualized as linear adsorbed material running from the top left to bottom right. **c,** An enlarged view of the rectangular region enclosed by the white dashed line in b (–2V, 5 pA, 100 nm). **d,** A *dI/dV* map of the same region as in **c** (–1.5 V, 20 pA, 100 nm). To maximize the detection of the density of states of guanine, the measurements were made under slightly lower bias conditions than in **c. e,** Part of the base sequence of M13mp18 obtained from a databank (the sequence of bases at positions 5322 through 5461). To facilitate comparison with the STM data, the guanine sites are indicated by red characters and are also connected by red arrows to the corresponding parts of the image.

Figure 1b shows a typical wide-region STM image (400 nm wide) of an ss M13mp18 extended and fixed by oblique injection on a Cu(111) surface. Owing to the height differences at steps in the substrate, the contrast is not ideal for recognizing DNA molecules, but it is possible to recognize two DNA strands running from left to right. Using this extended DNA, and to check whether or not it is possible to assign the individual guanine units, we measured topography images and *dI/dV* map images over the 100-nm-wide region highlighted in Fig. 1b. In the topography image of Fig. 1c, the individual nucleotides are shown as bright points, which are exceptionally bright in some places. The nucleotides that appeared brightest in the topography image also appear as clear bright points in the *dI/dV* map of Fig. 1d. For comparison, part of the known base sequence of M13mp18 is shown in Fig. 1e. The observed image and the known guanine sequence match almost perfectly, illustrating that STM can be used to sequence the guanine in real DNA.

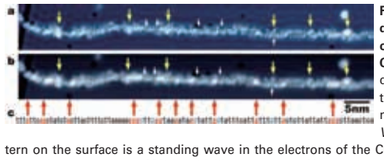

Fig.2 Bias voltage dependence on the STM imaging of M13mp18 DNA on a Cu(111) surface. a,b, Raw data obtained with the same tip on the same 70 nm × 9 nm area: Vs=0.1 V (**a**), and *Vs*=-2 V (**b**). The ripple pattern on the surface is a standing wave in the electrons of the Cu(111) surface. **c,** Part of the known base sequence of M13mp18 (the sequence of bases at positions 2911 to 3011). To facilitate comparison with the STM data, the guanine sites are indicated by red characters and are also connected by red arrows to the corresponding parts of the image. Some of the cytosine units are indicated by blue characters and the corresponding nucleotides in the STM images (**a**,**b**) are indicated by white arrows. The yellow arrows in the STM images indicate contaminants.

To make further advances towards the use of STM as a practical tool for sequencing, we must be able to recognize all four types of base molecule, and achieve greater speed and precision. In general, lock-in detection sacrifices temporal resolution for the sake of improved signal-to-noise ratio. If STM software and control mechanisms capable of finding chain-shaped polymers such as DNA can be developed, then the time taken to scan parts where the sample is not present can be greatly reduced. Savings in cost and time can also be made if sequencing is performed from the topographic image alone without using a lock-in amplifier, but it would still be necessary to use a method for identifying contamination. A method that is relatively fast and easy to implement involves comparing the STM bias dependence. That is, if guanine can be distinguished by comparing two images obtained at a value of *Vs* that is much lower than the peak in the density of states for guanine (for example, -2 V) and in fact at a value close to 0 V, then it should be possible to perform sequencing at high speed without the need for spectroscopy. As shown in Fig. 2, comparing images obtained at different bias voltages helps distinguish between DNA base molecules and contaminants: irregular points of brightness that do not vary with the bias voltage (yellow arrows in Fig. 2a) are contaminants.

The undulating pattern surrounding the DNA chain in Fig. 2a is observed at low bias conditions (*Vs* =0.1 V), and is thus a standing wave resulting from the scattering of surface electrons.[8] Compared with the image obtained with a low bias voltage, some of the nucleotides in the high bias image (*Vs*=-2 V) are brighter and thus correspond to guanine. To verify this, we compared the results with the sequence extracted from a databank (at positions 2911–3011) as shown in Fig. 2c, which can confirm if the guanine base molecules are completely matched either individually or in groups (g, gg, ggg). It can thus be seen that it is possible to recognize the guanine pattern with few errors simply by obtaining a pair of STM topographic images in this way (preferably dual bias mode). By closely examining the sections of the STM images of Fig. 2 where the nucleotides are neatly arranged, it appears as though the cytosine units are smaller than the thymine units (white arrows).

Fig.3 Example of pinpoint sequencing The false-colour STM image which measures 67 nm across, shows a DNA molecule running from bottom left to top right (the sequence of bases at positions 5084 to 5210; agaatgtccttttattactggtcgtgtgactggtgaatctgccaatgtaaataatccatttcagacgattgagcgtcaaaatgtaggtatttccatgagcgtttttcctgttgcaatggctggcgg). As can be seen, this STM image was featured on the cover of the journal. (http://www.nature.com/nnano/journal/v4/n8/covers/index.html)

Conclusions

In conclusion, by developing a method for extending and fixing DNA strands, we have taken a step towards the realization of electronic-based single-molecule DNA sequencing. Of the four bases, we were able to precisely identify guanine because the STM is able to pick up on the characteristics of its electronic state, which is largely independent of the adsorption structure. If vibrational spectroscopy is performed using inelastic electron tunnelling spectroscopy, it should be possible to identify all of the base molecules.[9] Furthermore, because STM can select a specific position of interest along a DNA strand, as shown in Fig.3, the technique could have a unique advantage in analysing, for example, single nucleotide polymorphisms.

References

[1] [1] D. Porath, *Nature Nanotech*. **4**, 476–477 (2009).
[2] C. R. Clemmer et al., *Science* **251**, 640–642 (1991).
[3] H. Tanaka et al., *J. Vac. Sci. Technol. B* **15**, 602–604 (1997).
[4] H. Tanaka et al., *Surf. Sci.* **432**, L611–L616 (1999).
[5] H. Tanaka et al., *Surf. Sci.* **539**, L531–L536 (2003).
[6] H. Tanaka et al., Japanese patent Kokoku 2005-46665 (2005).
[7] R. Ebright et al., *Gene* **114**, 81–83 (1992).
[8] M. F. Crommie et al., *Nature* **363**, 524–527 (1993).
[9] W. Ho, *J. Chem. Phys.* **117**, 11033–11061 (2002).

Zc3h12a is an RNase Essential for Controlling Immune Responses by Regulating mRNA Decay

Paper in journals : this is the first page of a paper published in ***Nature.***
[*Nature*] 458, 1185–1190 (2009)

Vol 458|30 April 2009|doi:10.1038/nature07924 nature

LETTERS

Zc3h12a is an RNase essential for controlling immune responses by regulating mRNA decay

Kazufumi Matsushita[1,3]*, Osamu Takeuchi[1,3]*, Daron M. Standley[2], Yutaro Kumagai[1,3], Tatsukata Kawagoe[1,3], Tohru Miyake[1,3], Takashi Satoh[1,3], Hiroki Kato[1,3], Tohru Tsujimura[4], Haruki Nakamura[5] & Shizuo Akira[1,3]

Toll-like receptors (TLRs) recognize microbial components, and evoke inflammation and immune responses[1–3]. TLR stimulation activates complex gene expression networks that regulate the magnitude and duration of the immune reaction. Here we identify the TLR-inducible gene *Zc3h12a* as an immune response modifier that has an essential role in preventing immune disorders. *Zc3h12a*-deficient mice suffered from severe anaemia, and most died within 12 weeks. *Zc3h12a*$^{-/-}$ mice also showed augmented serum immunoglobulin levels and autoantibody production, together with a greatly increased number of plasma cells, as well as infiltration of plasma cells to the lung. Most *Zc3h12a*$^{-/-}$ splenic T cells showed effector/memory characteristics and produced interferon-γ in response to T-cell receptor stimulation. Macrophages from *Zc3h12a*$^{-/-}$ mice showed highly increased production of interleukin (IL)-6 and IL-12p40 (also known as IL12b), but not TNF, in response to TLR ligands. Although the activation of TLR signalling pathways was normal, *Il6* messenger RNA decay was severely impaired in *Zc3h12a*$^{-/-}$ macrophages. Overexpression of Zc3h12a accelerated *Il6* mRNA degradation via its 3′-untranslated region (UTR), and destabilized RNAs with 3′-UTRs for genes including *Il6*, *Il12p40* and the calcitonin receptor gene *Calcr*. Zc3h12a contains a putative amino-terminal nuclease domain, and the expressed protein had RNase activity, consistent with a role in the decay of *Il6* mRNA. Together, these results indicate that Zc3h12a is an essential RNase that prevents immune disorders by directly controlling the stability of a set of inflammatory genes.

The innate immune responses induced by TLRs are tightly controlled, because aberrant activation of TLR responses is harmful to the host, resulting in inflammatory diseases[1–4]. TLR signalling induces the expression of several genes, although only some of these genes have been functionally characterized as immune response modifiers. Therefore, investigation of TLR-inducible genes is important for clarifying the control mechanisms of innate immune reactions. To examine TLR-induced gene expression comprehensively, we performed microarray analysis using mouse macrophages from wild-type, *Myd88*$^{-/-}$ and *Trif*$^{-/-}$ (also known as *Ticam1*$^{-/-}$) mice stimulated with lipopolysaccharide (LPS), a TLR4 ligand. We selected 214 genes in which the expression was induced more than twofold either at 1 or 4 h after stimulation in wild-type cells. Hierarchical clustering of these LPS-inducible genes showed that they could be classified into three major clusters (Supplementary Fig. 1a). Among the clusters, genes in cluster III were rapidly induced in a MyD88-dependent manner. This cluster contained, among others, *Tnf*, *Nfkbiz* and *Zfp36*. Cluster III also contained the gene encoding Zc3h12a (Supplementary Fig. 1b). Northern blot analysis confirmed that *Zc3h12a* mRNA was rapidly induced in mouse macrophages after LPS stimulation and gradually decreased with time (Supplementary Fig. 1c). Zc3h12a has a CCCH-type zinc-finger motif, and forms a family with the homologous proteins Zc3h12b, Zc3h12c and Zc3h12d. Fractionation experiments showed that the Zc3h12a protein is mainly localized in the cytoplasm, rather than in the nucleus (Supplementary Fig. 1d).

To investigate the functional roles of Zc3h12a in the control of immune responses *in vivo*, we generated *Zc3h12a*-deficient mice (Supplementary Fig. 2a and 2b). PCR with reverse transcription (RT–PCR) analysis confirmed that the expression of *Zc3h12a* was abrogated in *Zc3h12a*$^{-/-}$ macrophages (Supplementary Fig. 2c). Although *Zc3h12a*$^{-/-}$ mice are born in a Mendelian ratio, they showed growth retardation, and most of the mice spontaneously died within 12 weeks of birth (Fig. 1a). *Zc3h12a*$^{-/-}$ mice showed severe splenomegaly and lymphoadenopathy (Fig. 1b). Histological examination revealed infiltration of plasma cells in the lung, paraepithelium of the bile duct and pancreas (Fig. 1c and Supplementary Fig. 3). Plasma cells also accumulated in *Zc3h12a*$^{-/-}$ lymph nodes and spleens (Fig. 1c). In the lymph nodes, granuloma formation was observed leading to the generation of giant cells with fused macrophages. Nevertheless, inflammatory changes were not observed in either the intestine or the joints of *Zc3h12a*$^{-/-}$ mice (data not shown).

Zc3h12a$^{-/-}$ mice suffered from severe anaemia, together with an increase in white blood cells and platelets (Fig. 1d). Furthermore, *Zc3h12a*$^{-/-}$ mice developed hyperimmunoglobulinemia of all immunoglobulin isotypes tested (Fig. 1e), and plasma cells infiltrated in the lung interstitial tissues were readily stained with anti-IgG or anti-IgA antibodies (Fig. 1g). Production of anti-nuclear antibodies and anti-double-stranded-DNA antibodies were detected in *Zc3h12a*$^{-/-}$ mice (Fig. 1f). Flow cytometric analysis showed that about 70% of CD19$^+$ B cells were IgM$^-$ IgD$^-$, but immunoglobulin$^+$, indicating that most *Zc3h12a*$^{-/-}$ B cells underwent a class switch in the spleen (Fig. 2a and data not shown). Furthermore, CD138$^+$ CD19^{low} plasma cells were abundant in the spleen of *Zc3h12a*$^{-/-}$ mice (Fig. 2b). In addition, the expression of CD69 was upregulated in splenic CD3$^+$ T cells, and CD44^{high} CD62L$^-$ T cells accumulated in the periphery (Fig. 2c and Supplementary Fig. 4a). Nevertheless, the proportion of CD4$^+$ Foxp3$^+$ regulatory T cells was comparable between wild-type and *Zc3h12a*$^{-/-}$ mice (Supplementary Fig. 4b). Stimulation of splenic T cells with anti-CD3 antibody resulted in increased production of IFN-γ, but not IL-17 (Fig. 2d and Supplementary Fig. 4c). Ter119$^+$ (also known as Ly76$^+$) erythroblast population was higher in *Zc3h12a*$^{-/-}$ spleens, probably reflecting the responses to anaemia (Supplementary Fig. 4d). However, the ratios of B to T cells and of CD4$^+$ to CD8$^+$ cells were not altered in *Zc3h12a*$^{-/-}$ spleens (Supplementary Fig. 4e, f). To examine whether haematopoietic cells are sufficient for the development of disease, we transferred bone marrow cells from *Zc3h12a*$^{-/-}$ mice to recipient

[1]Laboratory of Host Defense, [2]Laboratory of Systems Immunology, WPI Immunology Frontier Research Center, [3]Research Institute for Microbial Diseases, Osaka University, 3-1 Yamada-oka, Suita, Osaka 565-0871, Japan. [4]Department of Pathology, Hyogo College of Medicine, 1-1 Mukogawa-cho, Nishinomiya, Hyogo 663-8501, Japan. [5]Research Center for Structural and Functional Proteomics, Institute for Protein Research, Osaka University, 3-2 Yamada-oka, Suita, Osaka 565-0871, Japan.
*These authors contributed equally to this work.

▲Reprinted with permission from ***Nature***, 458, 1185-1190(2009). Copyright 2009 Nature Publishing Group.

The following is a comment on the published paper shown on the preceding page.

Zc3h12a is an RNase Essential for Controlling Immune Responses by Regulating mRNA Decay

TAKEUCHI Osamu and AKIRA Shizuo
(Immunology Frontier Research Center)

Introduction

Toll-like receptors (TLRs) recognize microbial components, and evoke inflammation and immune responses. The innate immune responses induced by TLRs are tightly controlled, because aberrant activation of TLR responses is harmful to the host, resulting in inflammatory diseases[1-3]. TLR signalling induces the expression of several genes, although only some of these genes have been functionally characterized as immune response modifiers. Therefore, investigation of TLR-inducible genes is important for clarifying the control mechanisms of innate immune reactions. In this study, we identified Zc3h12a as a gene rapidly expressed in mouse macrophages in response to stimulation with lipopolysaccharide (LPS), a TLR4 ligand. Zc3h12a has a CCCH-type zinc-finger motif, and forms a family with the homologous proteins Zc3h12b, Zc3h12c and Zc3h12d. Fractionation experiments showed that the Zc3h12a protein is mainly localized in the cytoplasm, rather than in the nucleus. To investigate the functional roles of Zc3h12a in the control of immune responses *in vivo*, we generated *Zc3h12a*-deficient mice.

Zc3h12a prevents development of autoimmune diseases

Although *Zc3h12a*$^{-/-}$ mice are born in a Mendelian ratio, they showed growth retardation, and most of the mice spontaneously died within 12 weeks of birth (Fig. 1a). *Zc3h12a*$^{-/-}$ mice showed severe splenomegaly and lymphoadenopathy (Fig.1b). Histological examination revealed infiltration of plasma cells in the lung, paraepithelium of the bile duct and pancreas. Plasma cells also accumulated in *Zc3h12a*$^{-/-}$ lymph nodes and spleens. In the lymph nodes, granuloma formation was observed leading to the generation of giant cells with fused macrophages. *Zc3h12a*$^{-/-}$ mice developed hyperimmunoglobulinemia of all immunoglobulin isotypes tested, and plasma cells infiltrated in the lung interstitial tissues were readily stained with anti-IgG or anti-IgA antibodies. Production of anti-nuclear antibodies and anti-double-stranded-DNA antibodies were detected in *Zc3h12a*$^{-/-}$ mice (Fig.1c). Flow cytometric analysis showed that about 70% of CD19^{+} B cells were IgM^{-} IgD^{-}, but immunoglobulin^{+}, indicating that most *Zc3h12a*$^{-/-}$ B cells underwent a class switch in the spleen. Furthermore, CD138^{+}CD19^{dull} plasma cells were abundant in the spleen of *Zc3h12a*$^{-/-}$ mice. In addition, the expression of CD69 was upregulated in splenic CD3^{+} T cells, and CD44^{high} CD62L^{-} effector/memory T cells accumulated in the periphery.

These results demonstrate that Zc3h12a is essential for preventing the development of severe immune diseases characterized by an increase in immunoglobulin-producing plasma cells and the formation of granulomas.

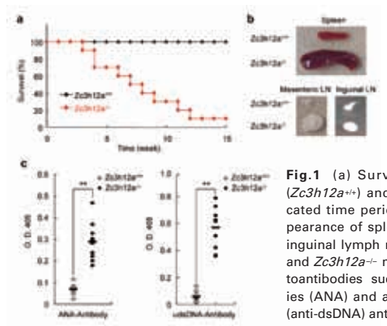

Fig.1 (a) Survival rates of wild-type (*Zc3h12a*$^{+/+}$) and *Zc3h12a*$^{-/-}$ mice at indicated time periods (n=10). (b) Gross appearance of spleens and mesenteric and inguinal lymph nodes (LN) from wild-type and *Zc3h12a*$^{-/-}$ mice. (c) Production of autoantibodies such as anti-nuclear antibodies (ANA) and anti-double-stranded DNA (anti-dsDNA) antibodies in *Zc3h12a*$^{-/-}$ mice.

Enhanced TLR-induced cytokine production by Zc3h12a deficiency

Since Zc3h12a is a TLR-inducible gene in macrophages, we examined the role of Zc3h12a in the responses of macrophages against TLR stimulation. Macrophages are known to produce proinflammatory cytokines in response to incubation with a set of TLR ligands. TLR ligands, MALP2 (TLR2), poly(I:C) (TLR3), LPS (TLR4), R848 (TLR7) and CpG DNA (TLR9) induced increased production of IL-6 and IL-12p40, but not of TNF, in *Zc3h12a*$^{-/-}$ macrophages (Fig.2). Northern blot analysis showed that *Il6* mRNA, but not *Tnf*, *Cxcl1* or *Ikba* mRNA, increased significantly in response to LPS in *Zc3h12a*$^{-/-}$ macrophages, indicating that Zc3h12a negatively regulates IL-6 and IL-12p40 mRNA expression.

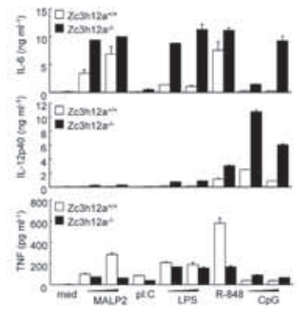

Fig.2 Peritoneal macrophages from wild-type and *Zc3h12a*$^{-/-}$ mice were stimulated with MALP-2 (1, 10 ng ml^{-1}), poly(I:C) (pI:C), 100 μg ml^{-1}), LPS (10, 100 ng ml^{-1}), R-848 (10 nM) and CpG DNA (0.1, 1 μM) for 24 h. The concentrations of IL-6, IL-12p40 and TNF in the culture supernatants were measured by ELISAs. Error bars indicate the s.d. of duplicates.

Zc3h12a controls Il6 mRNA decay

CCCH-type zinc-finger proteins have been implicated in mRNA metabolism such as mRNA splicing, polyadenylation and the regulation of mRNA decay[4]. Thus, we proposed that Zc3h12a might be involved in the destabilization of mRNA, and we examined this possibility using *Il6* as an example. Wild-type and *Zc3h12a*$^{-/-}$ macrophages were stimulated with LPS for 2 h followed by actinomycin D treatment. The half-life of *Il6* mRNA, but not of *Tnf* mRNA, increased in *Zc3h12a*$^{-/-}$ macrophages compared to wild-type cells (Fig.3). These results indicate that Zc3h12a regulates *Il6* mRNA post-transcriptionally. Reciprocally, we transfected HEK293 cells stably expressing the tetracycline repressor protein fused to the transactivation domain of the viral transcription factor VP-16 (Tet-off 293 cells), with a plasmid containing the *Il6* coding sequence (CDS) with the 3'-untranslated region (UTR) sequence under the control of a tetracycline-responsive promoter (TRE) (pTREtight-Il6-CDS + 3'-UTR). Treatment with doxycycline (dox) terminated the transcription of *Il6* mRNA, and the mRNA decayed in an incubation time-dependent manner. Overexpression of Zc3h12a greatly accelerated the degradation of *Il6* mRNA. In contrast, Zc3h12a did not affect the expression of mRNA harbouring the *Il6* CDS without the 3'-UTR sequence (pTREtight-Il6-CDS). Taken together, Zc3h12a controls Il6 mRNA stability through its 3'-UTR.

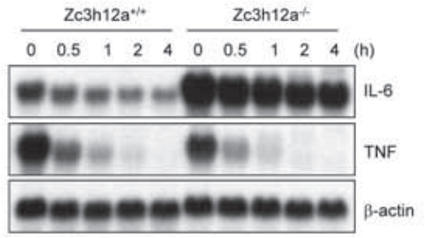

Fig.3 Peritoneal macrophages were treated with LPS (100 ng ml^{-1}) for 120 min and then treated with actinomycin D (2 μg ml^{-1}) for the indicated times. Total RNA (10 μg) was extracted and subjected to RNA blot analysis for the expression of *Il6*, *Tnf*, *KC* and β-actin (*Actb*) probes.

Zc3h12a has an RNase activity responsible for controlling Il6 mRNA stability

Then we investigated the mechanism how Zc3h12a negatively regulate mRNA stability. Sequence alignment indicated that a conserved N-terminal domain (139–297) in Zc3h12a, just preceding the zinc-finger domain (300–324), shares remote homology to the PilT N-terminus (PIN) domain-like Structural Classification of Proteins (SCOP) superfamily. Structural modelling, followed by alignment to other PIN domain structures, revealed a conserved, negatively charged pocket—formed by Asp 141, Asn 144, Asp 226, Asp 244 and Asp 248—that is potentially important for magnesium binding and enzymatic activity (Fig.4a). We proposed that the N-terminal domain of the Zc3h12a protein might be an RNase, and synthesized Zc3h12a protein showed RNase activity for *Il6* 3'-UTR (1–403) mRNA in an Mg^{2+}-dependent manner (Fig.4b). Furthermore, the Zc3h12a(D141N) mutant did not degrade RNA, indicating that the conserved pocket indeed functions as an RNase active site (Fig.4b). The Zc3h12a(D141N) mutant failed to destabilize RNA containing the *Il6* 3'-UTR in HEK293 cells, indicating that the RNase activity is essential for the function of Zc3h12a (Fig. 4c, d).

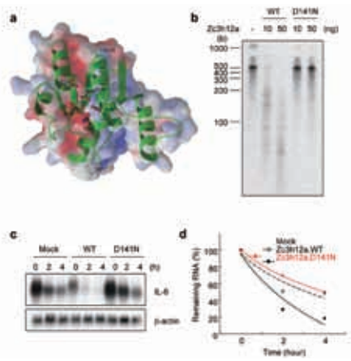

Fig.4 (a) The structural model of the Zc3h12a N-terminal domain. (b) The RNase activity of Zc3h12a and Zc3h12a(D141N) proteins in degrading *Il6* 3'-UTR mRNA (1–403) in the presence or absence of 5 mM Mg^{2+}. (c) HEK293 Tet-off cells were cotransfected with pTREtight-Il6 full, and Zc3h12a or Zc3h12a(D141N). The cells were then treated with dox for the indicated periods and *Il6* expression was determined by northern blot analysis. (d) The autoradiograph shown in (c) was quantified and the ratio of *Il6* to *Actb* was used to determine remaining mRNA levels.

Conclusion

In the present study, we show that the Zc3h12a protein has intrinsic RNase activity responsible for the decay of *Il6* mRNA. The mechanism is unique compared to the regulation of other AU rich element (ARE)-mediated mRNA decay pathways. For instance, Tristetraprolin has been shown to recruit deadenylases for removing polyA tails, facilitating the subsequent degradation of target mRNAs by exonucleases [4]. Thus, it is intriguing that Zc3h12a has endonuclease activity, which, at least *in vitro*, does not show sequence specificity. The target specificity may be determined by binding partner(s) of Zc3h12a, or Zc3h12a may have a preferential sequence for degradation under certain conditions. The mechanism of how Zc3h12a induces decay of mRNAs is an intriguing topic for further exploration.

Given that each CCCH zinc-finger protein seems to have target mRNA specificity and 60 CCCH-type zinc-finger proteins have been identified in the mammalian genome[5], control of mRNA decay might be as important as the control of transcription in terms of regulation of innate immune responses. Future studies on CCCH zinc-finger proteins will be important for understanding the mechanisms of immune regulation by the control of mRNAs.

References

[1] Takeuchi, O. & Akira, S. Pattern recognition receptors and inflammation. *Cell* **140**, 805-820 (2010).
[2] Beutler, B. et al. Genetic analysis of resistance to viral infection. *Nat Rev Immunol* **7**, 753-766 (2007).
[3] Medzhitov, R. Recognition of microorganisms and activation of the immune response. *Nature* **449**, 819-826 (2007).
[4] Anderson, P. Post-transcriptional control of cytokine production. *Nat Immunol* **9**, 353-359 (2008).
[5] Liang, J., Song, W., Tromp, G., Kolattukudy, P.E. & Fu, M. Genome-wide survey and expression profiling of CCCH-zinc finger family reveals a functional module in macrophage activation. *PLoS ONE* **3**, e2880 (2008).